Molecular Dynamics of Staphylococcal Nuclease: Comparison of Simulation with ^{15}N and ^{13}C NMR Relaxation Data

David C. Chatfield,*,† Attila Szabo,‡ and Bernard R. Brooks§

Contribution from the Chemistry Department, Florida International University, Miami, Florida 33199, and Laboratory of Structural Biology, Division of Computer Research and Technology, and Laboratory of Chemical Physics, National Institute of Diabetes and Digestive and Kidney Diseases, National Institutes of Health, Bethesda, Maryland 20892

Received July 3, 1997. Revised Manuscript Received October 16, 1997

Abstract: Motional parameters for the atomic-level dynamics of staphylococcal nuclease are calculated from an 18-ns molecular dynamics simulation of the liganded enzyme and from a 3.75-ns simulation of the unliganded enzyme and compared with motional parameters calculated from ^{13}C and ^{15}N NMR relaxation data. Order parameters for backbone N−H and C_α−H bond vectors are on average in good agreement with experiment, indicating a similar degree of backbone flexibility. Somewhat greater flexibility is seen in the simulation of unliganded SNase, consistent with some experimental data. Alanine C_α−C_β and C_α−H order parameters agree to within 5% for simulation while NMR finds the former to be 30% smaller than the latter; thus experimental reexamination of $^{13}CH_3$ relaxation may be worthwhile. Average simulated and experimental rotation rates for the more rapidly rotating alanine and leucine methyl groups are in agreement. However, simulation predicts a much larger range of methyl rotation rates than is observed experimentally. Analysis of methyl rotations in a variety of environments indicates that the variation in the simulated methyl rotation rates is due to steric (van der Waals) interactions.

Introduction

Recent progress in NMR spectroscopy has begun to provide an atomic-level description of protein dynamics and structure in solution. Such a view is a valuable complement to X-ray crystallography, which provided the first atomic-level view of proteins but is restricted to static structures in crystalline matrixes. Two-dimensional (2D) heteronuclear NMR techniques that allow one to accurately measure nuclear spin relaxation of ^1H, ^{15}N, and ^{13}C nuclei yield a detailed description of protein backbone and side-chain motions.[1−4] Recent studies of staphylococcal nuclease (SNase) demonstrate the capabilities of such an approach.[5−8]

Molecular dynamics (MD) simulations of SNase, reported here, were performed to complement the 2D NMR studies. Of particular interest are generalized order parameters (S) and relaxation times (τ), which quantify the extent and time scale of motions of particular bonds.[9] The ^{13}C and ^{15}N relaxations measured by NMR are primarily determined by the motions of the corresponding C−H and N−H bond vectors. The 2D NMR studies focus on the dynamics of backbone N−H and C_α−H bonds and bonds in alanine (Ala) and leucine (Leu) methyl groups. The MD simulations address the following questions: How well do experimental and simulated order parameters compare for the protein backbone? For the side-chain methyls? How well do relaxation times compare? How does ligand binding affect the motional characteristics?

Additionally, in light of discrepancies between simulation and experiment, the validity of several assumptions often made in the analysis of NMR relaxation data were tested: that ideal tetrahedral geometry can be assumed for side-chain methyls, that calcuating order parameters using average values for the bond lengths is accurate, and that only protons directly bonded to a heteronucleus contribute to the NMR signal significantly. Finally, assumptions concerning the relationship between the ^{15}N chemical shift anisotropy and the ^{15}N−^1H dipolar interaction were also investigated.

Some of the previous simulation work on the influence of protein motions on structural and dynamical information calculated from NMR data is summarized below. Order parameters for the symmetry axes of several methyl groups in BPTI, extracted from ^{13}C NMR relaxation data, were compared[10] with those calculated from a 96-ps simulation. The effects of motional averaging on structural information obtained from ^1H NOE data were assessed on the basis of a 33-ps MD trajectory

† Florida International University.
‡ Laboratory of Chemical Physics, National Institutes of Health.
§ Laboratory of Structural Biology, National Institues of Health.

(1) Kay, L. E.; Torchia, D. A.; Bax, A. *Biochemistry* **1989**, *28*, 8972.
(2) Clore, G. M.; Szabo, A.; Bax, A.; Kay, L. E.; Driscoll, P. C.; Gronenborn, A. M. *J. Am. Chem. Soc.* **1990**, *112*, 4989−4991.
(3) Clore, G. M.; Driscoll, P. C.; Wingfield, P. T.; Gronenborn, A. M. *Biochemistry* **1990**, *29*, 7387.
(4) Palmer, A. G., III; Rance, M.; Wright, P. E. *J. Am. Chem. Soc.* **1991**, *113*, 4371.
(5) Nicholson, L. K.; Kay, L. E.; Baldisseri, D. M.; Arango, J.; Young, P.; Bax, A.; Torchia, D. A. *Biochemistry* **1992**, *31*, 5253−5263.
(6) Torchia, D. A.; Nicholson, L. K.; Cole, H. B. R.; Kay, L. E. In *Topics in Molecular and Structural Biology*; Clore, G. M.; Gronenbaum, A. M., Eds.; MacMillan: London, 1993; pp 190−219.
(7) Nicholson, L. K.; Kay, L. E.; Torchia, D. A. In *NMR Spectroscopy and its Application to Biomedical Research*; Sarkar, S. K., Ed.; Elsevier: New York, 1996; pp 241−279.
(8) Alexandrescu, A. T.; Jahnke, W.; Wilscheck, R.; Blommers, M. J. J. *J. Mol. Biol.* **1996**, *260*, 570−587.
(9) Lipari, G.; Szabo, A. *J. Am. Chem. Soc.* **1982**, *104*, 4546−4559.
(10) Lipari, G.; Szabo, A.; Levy, R. M. *Nature* **1982**, *300*, 197−198.

S0002-7863(97)02215-4 CCC: $15.00
Published on Web 05/19/1998

of lysozyme using an extended atom model.[11] The effects of motional averaging on ring-current contributions to proton chemical shifts and on vicinal proton spin−spin coupling constants were studied with MD simulations of bovine pancreatic trypsin inhibitor and lysozyme.[12] A 500-ps MD simulation study of solvated interleukin-1β compared calculated and NMR backbone N−H order parameters to suggest a molecular picture of the slow internal motions inferred from NMR data.[13] The influence of fast angular and radial intramolecular dynamics on NMR cross-relaxation rates was analyzed on the basis of an 800-ps MD simulation of a cyclic decapeptide in chloroform.[14] The effects of internal motion on dipolar nuclear magnetic relaxation of C−H, N−H, and H−H spin pairs were assessed on the basis of 100-ps simulations of a 25-residue zinc-finger peptide, good agreement with NMR being obtained for fast ($<$10 ps) motions.[15] The last simulation was also used to develop a model for interpreting NMR relaxation data in terms of a normal mode description of protein motion.[16]

SNase is a 149-residue bacterial enzyme that leaves DNA and RNA. SNase is an ideal candidate for study because it is small, contains no disulfide bridges or sulfydryl groups, and possesses considerable thermostability. Furthermore, a large body of experimental work on SNase exists. SNase is considered a prime model for studying enzyme mechanism and protein folding. The interested reader is referred to other work on SNase, including extensive reviews,[17,18,19,20] for further discussion of its physical properties,[17,18] the structure of the active site,[18,21,22,23] likely reaction mechanisms,[19,21,24] folding studies,[8,20,25] and site-directed mutagenesis studies.[26,27]

Simulations were performed for SNase in liganded and unliganded forms, both of which were also studied with 2D NMR. Starting coordinates for simulation were X-ray crystal structures of the unliganded enyme[23] or the ternary complex[22] with deoxythymidine 3′,5′-diphosphate (dpTp) and a single Ca^{2+} ion. In the following, unless otherwise stated, experimental data for the dynamics of N−H bond vectors correspond to ref 6 and recent reanalysis of data presented therein, and data for alanine and leucine methyl bond vectors are taken from ref 7.

Methods

Simulations. The MD simulations were performed with CHARMM,[28] using the PARM30 parameter set[29,30] with modifications to certain methyl torsion parameters described in the Appendix. PARM30 was the only CHARMm parameter set available for treating both peptides and nucleotides at the time these simulations were begun. Waters were represented with a modified[31] TIP3P model,[32] and a constant dielectric ($\epsilon = 1$) was used. Electrostatic forces were treated with the force switch method with a switching range of 8−12 Å. van der Waals forces were treated with the shift method with a 12-Å cutoff.[33] Nonbond lists were kept to 14 Å and updated heuristically. Hydrogens were placed with the HBUILD routine[34] of CHARMM, and the dynamics was propogated with the Verlet leapfrog algorithm using a time step of 1 fs.

Initial structures were the X-ray crystallographic coordinates of refs 22 and 23 for liganded and unliganded SNase, respectively. In both cases, residues 1−6 and 142−149 were deleted for the simulation because they are disordered and poorly resolved in the crystal structure. It has been demonstrated that SNase activity is unimpaired by the deletion of residues 1−6[18,19,35−37] and is retained, although somewhat diminished, when residues 142−149 are deleted.[19,38−40]

To simulate the solvated state, one would ideally place the protein in a large box of water and apply periodic boundary conditions. To generate a simulation trajectory of sufficient length to sample certain motions (in particular, the rotation of Ala and Leu methyl groups), it was necessary to restrict the size of the modeled system. Therefore, SNase was hydrated with a moderate number of water molecules. The crystal structures for liganded and unliganded SNase include 82 and 85 waters, respectively. Additional waters were added for simulation, using a protocol developed previously[41] and outlined below, bringing the total number to 350 for liganded and 369 for unliganded SNase. The additional waters for unliganded SNase are needed to fill the ligand binding site. For myoglobin, such a minimal solvation layer hydrates surface charged groups and yields a conformation and fluctuations on the 100-ps time scale comparable to those obtained in simulations with 3830 waters.[31] This level of hydration corresponds to the hydrated powder form of proteins used in Mössbauer spectroscopy.

Initial coordinates for the solvent waters were assigned by placing the SNase system in a large, equilibrated box of waters and deleting all waters except those with oxygens (1) at least 2.5 Å from the nearest nuclease, ligand, Ca^{2+}, or crystallographic water heavy atom and (2) not more than 3.855 Å (for liganded SNase) or 3.969 Å (for unliganded SNase) from the nearest nuclease, ligand, or Ca^{2+} heavy atom. Each system then had a total of 350 waters. For unliganded SNase, an additional 19 waters in the binding cleft whose oxygens satisfied criterion 1 were retained. The structure was then briefly energy-minimized (10 steps) to relieve bad crystal contacts.

The SNase systems were equilibrated in three stages. First, all atoms except solvent waters were restrained to their minimized positions by harmonic restraints having a force constant of 1 kcal/mol·Å^2, and 10 ps of dynamics was run to allow solvent waters to assume favorable

(11) Olejniczak, E. T.; Dobson, C. M.; Karplus, M.; Levy, R. M. *J. Am. Chem. Soc.* **1984**, *106*, 1923−1930.
(12) Hoch, J. C.; Dobson, C. M.; Karplus, M. *Biochemistry* **1985**, *24*, 3831−3841.
(13) Chandrasekhar, I.; Clore, G. M.; Szabo, A.; Gronenborn, A. M.; Brooks, B. R. *J. Mol. Biol.* **1992**, *226*, 239−250.
(14) Bruschweiler, R.; Roux, B.; Blackledge, M.; Griesinger, C.; Karplus, M.; Ernst, R. R. *J. Am. Chem. Soc.* **1992**, *114*, 2289−2302.
(15) Palmer, A. G., III; Case, D. A. *J. Am. Chem. Soc.* **1992**, *114*, 9059−9067.
(16) Bruschweiler, R.; Case, D. A. *Phys. Rev. Lett.* **1994**, *72*, 940−943.
(17) Tucker, P. W.; Hazen, E. E., Jr.; Cotton, F. A. *Mol. Cell. Biochem.* **1978**, *22*, 67−77.
(18) Tucker, P. W.; Hazen, E. E., Jr.; Cotton, F. A. *Mol. Cell. Biochem.* **1979**, *23*, 3−16.
(19) Tucker, P. W.; Hazen, E. E., Jr.; Cotton, F. A. *Mol. Cell. Biochem.* **1979**, *23*, 67−86.
(20) Tucker, P. W.; Hazen, E. E., Jr.; Cotton, F. A. *Mol. Cell. Biochem.* **1979**, *23*, 131−141.
(21) Cotton, F. A.; Hazen, E. E.; Legg, M. J. *Proc. Natl. Acad. Sci. U.S.A.* **1979**, *76*, 2551−2555.
(22) Loll, P. J.; Lattman, E. E. *Proteins: Struct., Funct., Genet.* **1989**, *5*, 183−201.
(23) Hynes, T. R.; Fox, R. O. *Proteins: Struct., Funct., Genet.* **1991**, *10*, 92−105.
(24) Serpersu, E. H.; Shortle, D.; Mildvan, A. S. *Biochemistry* **1987**, *26*, 1289−1300.
(25) Carra, J. H.; Anderson, E. A.; Privalov, P. L. *Biochemistry* **1994**, *33*, 10842−10850.
(26) Chuang, W.-J.; Weber, D. J.; Gittis, A. G.; Mildvan, A. S. *Proteins: Struct., Funct., Genet.* **1993**, *17*, 36−48.
(27) Wu, P.; Brand, L. *Biochemistry* **1994**, *33*, 10457−10462.
(28) Brooks, B. R.; Bruccoleri, R. E.; Olafson, B. D.; States, D. J.; Swaminathan, S.; Karplus, M. *J. Comput. Chem.* **1982**, *4* (2), 187−217.
(29) Parameter File for CHARMM Version 21, Molecular Simulation Inc., Burlington, MA, released May 22, 1990.
(30) Momany, F. A.; Rone, R. *J. Comput. Chem.* **1992**, *13*, 888−900.
(31) Steinbach, P. J.; Brooks, B. R. *Proc. Natl. Acad. Sci. U.S.A.* **1993**, *90*, 9135−9139.
(32) Jorgensen, W. L.; Chandrasekhar, J.; Medura, J. D.; Impey, R. W.; Klein, M. L. *J. Chem. Phys.* **1983**, *79*, 926−935.
(33) Steinbach, P. J.; Brooks, B. R. *J. Comput. Chem.* **1994**, *15*, 667.
(34) Brünger, A.; Karplus, M. *Proteins: Struct., Funct., Genet.* **1988**, *4*, 148−156.
(35) Taniuchi, H.; Anfinsen, C. B.; Sodja, A. *Proc. Natl. Acad. Sci. U.S.A.* **1967**, *58*, 1235.
(36) Taniuchi, H.; Anfinsen, C. B. *J. Biol. Chem.* **1968**, *243*, 4778.
(37) Schechter, A. N.; Moravek, L.; Anfinsen, C. B. *Proc. Natl. Acad. Sci. U.S.A.* **1968**, *61*, 1478.
(38) Arnone, A.; Bier, C. J.; Cotton, F. A.; Hazen, E. E., Jr.; Richardswon, D.; Richardson, J. S. *Proc. Natl. Acad. Sci. U.S.A.* **1971**, *64*, 1969.
(39) Taniuchi, H.; Anfinsen, C. B. *J. Biol. Chem.* **1969**, *244*, 3864.
(40) Parikh, I.; Corley, I.; Anfinsen, C. B. *J. Biol. Chem.* **1971**, *246*, 7392.
(41) Loncharich, R. J.; Brooks, B. R. *J. Mol. Biol.* **1990**, *215*, 439−455.

positions. Velocities were periodically reassigned to maintain a temperature of 300 K. Next, restraints were removed from X-ray waters, and another 10 ps of dynamics was run. Finally, all restraints were removed and the system was subjected to 30 ps of dynamics. Following equilibration, 300 K MD was performed at constant energy. The total simulation time was 18 ns for liganded and 3.75 ns for unliganded SNase. Prior to analysis of trajectories for motional parameters, overall translation and rotation of SNase was removed so that correlation functions describe internal motions only. The separability of correlations functions for overall tumbling and for internal motions is assumed.[9]

Order Parameters and Relaxation Times. Generalized order parameters and relaxation times were calculated for selected pairs of bonded atoms. The angular correlation function $C_I(t)$ describing the dynamics of, for example, an N−H bond is defined as

$$C_I(t) = \langle P_2(\hat{\mu}(\tau)\cdot\hat{\mu}(\tau + t))\rangle \quad (1)$$

where $\hat{\mu}$ is a unit vector pointing along the N−H bond and $P_2(x) = (3x^2/2 - {}^1/_2)$ is the second Legende polynomial. The square of the generalized order parameter (S^2) is defined as the long-time limit of C_I

$$S^2 = \lim_{t\to\infty} C_I(t) \quad (2)$$

Squared order parameters were calculated from simulations as the following time (equilibrium) average:[42,43]

$$S^2 = {}^3/_2[\langle x^2\rangle^2 + \langle y^2\rangle^2 + \langle z^2\rangle^2 + 2\langle xy\rangle^2 + 2\langle xz\rangle^2 + 2\langle yz\rangle^2] - {}^1/_2 \quad (3)$$

where x, y, and z are the projections of $\hat{\mu}$ on the x, y, and z axes. Equations 3 and 4 give identical results only when the trajectory is sufficiently long for the correlation function to have converged.

Relaxation times τ are defined by[9]

$$\tau = \frac{1}{1-S^2}\int_0^\infty (C_I(t) - S^2)\, dt \quad (4)$$

Values for τ were calculated for Ala and Leu methyl rotations by numerically integrating $C_I(t)$. Because the simulations are of limited duration, some correlation functions were not converged and manifested oscillations continuing to long time (i.e., these methyls were undergoing slow rotational reoriention). While it is not possible to rigorously obtain a correlation time for such "slow" methyls, we did obtain a rough estimate by integrating from $t = 0$ to the first time C_I reached 0.111, the theoretical value of S^2 for a methyl group with ideal tetrahedral geometry, as discussed below. The standard error in τ, σ_m, was estimated as

$$\sigma_m = \sqrt{2\tau/T} \quad (5)$$

where T is the simulation length.[44]

To evaluate the error introduced by using average bond lengths to extract order parameters from NMR data, we define functions $F_r(t)$ and $\hat{S}^2$ by

$$F_r(t) = \left\langle \frac{P_2(\hat{\mu}(\tau)\cdot\hat{\mu}(\tau + t))}{r^3(\tau)r^3(\tau + t)} \right\rangle \quad (6)$$

and

$$\hat{S}^2 = \langle r^{-3}\rangle^{-2} \lim_{t\to\infty} F_r(t) \quad (7)$$

where r is the interatomic distance. $\hat{S}^2$ is what is really extracted from NMR data if hydrogens not bonded directly to the heteronucleus contribute negligibly to the NMR signal. It is usually assumed that the difference between S^2 and $\hat{S}^2$ is insignificant. To test this assumption, $\langle r^{-3}\rangle^{-2}$ was calculated from the simulation $\hat{S}^2$ was and compared with S^2.

To test the assumption that hydrogens not bonded to the heteronucleus contribute negligibly to order parameters calculated from NMR data, we define a function $\hat{F}_r(t)$:

$$\hat{F}_r(t) = \sum_{r_i} F_{r_i}(t) \quad (8)$$

where the sum is over all hydrogens, and r_i is the distance of hydrogen i from the heteronucleus of interest. Replacing F_r in eq 7 with $\hat{F}_r$ yields order parameters that correspond to those extracted from NMR data under the aforementioned assumption.

Model free order parameters can be interpreted in terms of particular kinds of motions. Relationships pertinent to this study are given here. The reader is directed elsewhere for a more thorough discussion.[2,45] Diffusion of a bond vector $\hat{\mu}$ within a cone of semiangle θ, a reasonable model for the fast motions of backbone N−H and C_α−H bond vectors, yields the relationship:

$$S^2_{\text{cone}} = [{}^1/_2(\cos\theta)(1 + \cos\theta)]^2 \quad (9)$$

For an ideal methyl group having equivalent and constant C−H bond lengths and H−C−H bond angles and rotating about a stationary symmetry axis, the order parameter for motion of the C−H bond vector is given by

$$S^2_{\text{rot}} = [(3\cos^2\beta - 1)/2]^2 \quad (10)$$

where β is the angle with the symmetry axis. This relationship holds for both free diffusion about the symmetry axis and jumps among three equivalent sites about the symmetry axis. When β is 109.5°, S^2_{rot} is 0.111. For a methyl group exhibiting axially symmetric motion, the overall order parameter, S, is related to the order parameters for motion of the symmetry axis, S_{axis}, and rotation about the symmetry axis, S_{rot}, by

$$S^2 = S^2_{\text{rot}} S^2_{\text{axis}} \quad (11)$$

as long as motions of the axis and about the axis are uncoupled. This relationship is generally used for interpreting NMR data; i.e., tetrahedral geometry is assumed, and S^2_{axis} is calculated by dividing the measured squared order parameter for motion of the C−H bond vector by 0.111.

For the methyl groups of longer aliphatic chains such as leucine, more complicated motions must be considered.[45] In the simplest model that describes the motion of the symmetry axis of a leucine methyl (i.e., the C_γ−C_δ bond), dihedral fluctuations about the C_β−C_γ bond are superimposed upon the wobbling of the C_α−C_β bond. Assuming these motions are independent, and for small amplitude dihedral motions, the C_γ−C_δ order parameter, $S_{\gamma\delta}$, is given by[46]

$$S^2_{\gamma\delta} = S^2_{\alpha\beta}[1 - 3\langle(\Delta\phi)^2\rangle \sin^2\psi] \quad (12)$$

where $S_{\alpha\beta}$ is the C_α−C_β order parameter, $\langle(\Delta\phi)^2\rangle$ is the mean square fluctuation in the C_α−C_β−C_γ−C_δ dihedral angle, ϕ, and ψ is the C_β−C_γ−C_δ angle.

Results

The root-mean-square deviation (rmsd) of the atomic coordinates during simulation from the X-ray coordinates is shown in Figure 1 for liganded SNase. The lower curve is for backbone heavy (non-hydrogen) atoms; the upper curve is for all heavy atoms. The rmsd rises from 0 to about 4 ns and then stays relatively constant until about 15 ns, after which a shift occurs. The period from 4 to 15 ns was used for analysis. A 3.75-ns

(42) Henry, E.; Szabo, A. *J. Chem. Phys.* **1985**, *82*, 4753.
(43) Pastor, R. W.; Venable, R. M. In *Computer Simulation of Biomolecular Systems*; Gunsteren, W. F.v.; Weiner, P. K.; Wilkinson, A. J., Eds.; ESCOM: Leiden, 1993; Vol. 2, p 451.
(44) Zwanzig, R.; Ailawasi, N. *Phys. Rev.* **1969**, *182*, 280.
(45) Lipari, G.; Szabo, A. *J. Am. Chem. Soc.* **1982**, *104*, 4559−4570.
(46) Tjandra, N.; Szabo, A.; Bax, A. *J. Am. Chem. Soc.* **1996**, *118*, 6986−6991 (see eq A.6).

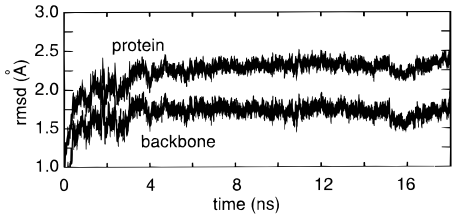

Figure 1. Root-mean-square deviation (rmsd) vs crystal structure during dynamics of liganded SNase. Lower curve is for backbone heavy atoms only (N, C_α, and C), and upper curve is for all heavy atoms.

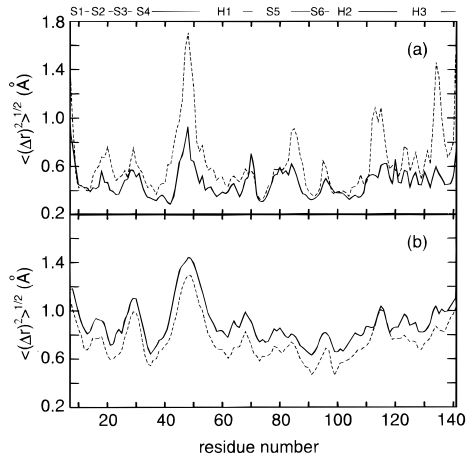

Figure 2. Root-mean-square atomic fluctuations averaged over backbone heavy atoms. Solid is for liganded SNase, and dashed is for unliganded SNase. (a) Simulation. (b) Calculated from experimental Debye−Waller factors[22,23] (eq 13). Secondary structure as identified for liganded SNase in ref 22 is indicated at the top. β-sheets are labeled S*X* and helices are labeled H*X*, where *X* is an integer, and a solid line indicates a turn or loop.

simulation was performed for unliganded SNase. The rmsd vs the crystal coordinates was comparable to that for liganded SNase, but the equilibration period was shorter, consistent with the unliganded protein being more flexible. The region of relatively stable rmsd from 1.75 to 3.75 ns was used for analysis.

Root-mean-square (rms) atomic fluctuations of backbone heavy atoms, averaged within a residue, are shown in Figure 2a. Trends in mobility are consistent with X-ray crystallographic rms atomic fluctuations,[22,23] shown in Figure 2b and calculated from the experimental *B* factors using[47]

$$B = \frac{8\pi^2}{3}\langle(\Delta r)^2\rangle \qquad (13)$$

Secondary structure is indicated at the top of Figure 2. The labeling of β-sheets and α-helices is consistent with ref 22. The reduced *B* values for unliganded relative to liganded SNase are likely due to crystal packing forces. Other experimental data, including liganded SNase's higher thermal unfolding temperature,[48] smaller amide proton exchange rate,[48] and larger NMR Ala $C_\alpha-C_\beta$ and Leu $C_\gamma-C_\delta$ methyl order parameters,[5,7] suggest that the extent of motion is greater in unliganded SNase.

Mobility of the backbone during simulation of liganded SNase is depicted by Figure 3, in which coordinates averaged over 0.5-ns intervals are overlaid. Medium gray, light gray, and black lines represent the crystal structure, the initial equilibration period, and the period used for analysis, respectively. Examples

(47) McCammon, J. A.; Harvey, S. C. *Dynamics of Proteins and Nucleic Acids*; Cambridge University Press: New York, 1987.
(48) Baldisseri, D. M.; Torchia, D. A. Unpublished results.

Figure 3. Overlays of backbone skeleton (N, C_α, and C) during dynamics of liganded SNase, shown in stereo for wall-eyed viewing (rotate page 90° for proper viewing). Each structure corresponds to coordinates averaged over a 0.5-ns window. Structures from the equilibration phase (1−4 ns) are shown in light gray, structures from the portion of the trajectory used for analysis are shown in black, and the crystal structure is shown in medium gray. The last 3 ns of simulation, which were not used for analysis, are not represented.

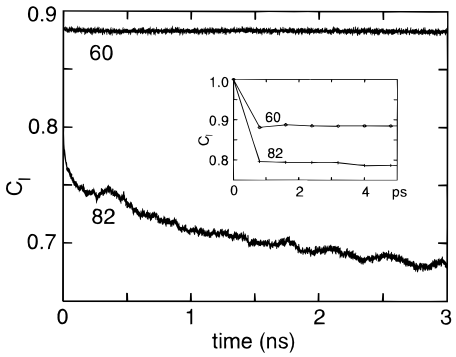

Figure 4. Correlation functions (C_I (t)) for two representative N−H bonds from the simulation of liganded SNase. Residue 60 is typical of most, but some, like residue 82, exhibit motion on the nanosecond time scale and are not converged or are barely converged in the 11 ns of simulation. The inset expands the short-time region to show the initial rapid decay.

of correlation functions for liganded SNase backbone N−H bond vectors are shown in Figure 4. The correlation function for residue 60, in helix 1, rapidly converges to 0.88, indicating restricted motion. The correlation function for residue 82, near the end of β-strand 5, converges more slowly and to a smaller value, indicative of greater mobility. The short-time dynamics is shown in the inset. Simulated and experimental[6] order parameters for backbone N−H bond vectors are shown in Figure 5.

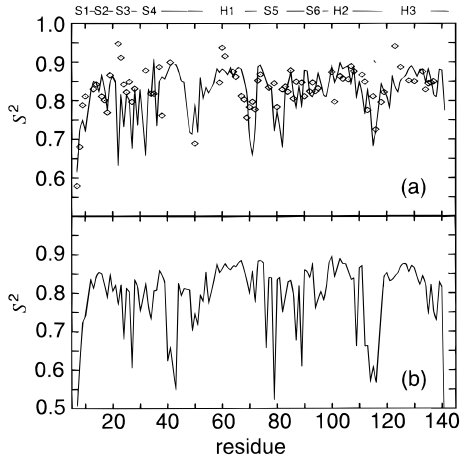

Figure 5. Squared generalized order parameters (S^2) for backbone N−H bond vectors for (a) liganded and (b) unliganded SNase. The solid lines are from simulation, and the diamonds in a are from experiment.[6] Secondary structure as identified for liganded SNase in ref 22 is indicated at the top. β-sheets are labeled S*X* and helices are labeled H*X* in accord with Figure 3, and a solid line indicates a turn or loop.

Table 1. Alanine C_β−H Relaxtion Times τ (ps)[a]

	liganded			unliganded		
residue	τ_{exp}[b]	τ_{sim}[b]	$\langle t_{res}\rangle$[c]	τ_{exp}	τ_{sim}	$\langle t_{res}\rangle$
12	27(1)	7.5(0.3)	14	30(2)	10(1)	13
17	29(1)	450(130)	520	28(4)	11(1)	19
58	55(3)	590(200)	740		49(11)	71
60	24(3)	23(1)	35	29(2)	46(10)	27
69	25(1)	280(60)	110	29(3)	100(30)	140
90	32(2)	36(3)	63	36(2)	12(1)	20
94	16(1)	220(40)	280	15(1)	21(3)	26
102	35(2)	130(20)	180		50(11)	65
109	21(2)	1100(500)	1600	31(3)	130(50)	140
112	16(2)	72(8)	140	22(3)	47(10)	51
130	21(1)	38(3)	67	22(1)	17(2)	21
132	50(7)	28(2)	57	58(2)	35(7)	49

[a] Where there is no value for simulation, the correlation function was not sufficiently converged for calculation of τ. [b] τ_{exp} and τ_{sim} are the relaxation times from the experiments of Nicholson et al.[7] and simulation, respectively. Numbers in parentheses are one standard deviation as calculated by Monte Carlo procedure for NMR data,[47] and estimates of the standard error from eq 5 for the simulation data. [c] $\langle t_{res}\rangle$ is the average time between rotations of a methyl across its 3-fold barrier in simulation.

Correlation functions for Ala and Leu methyl C−H bond vectors converge more slowly than those for backbone N−H vectors. The time scale for methyl rotations was quantified both by calculating the correlation time τ as described previously and by counting the number of times a methyl group crossed its 3-fold rotational barrier during simulation, including only crossings beginning at least 20° before and proceeding to at least 20° beyond the barrier. Average residence times, $\langle t_{res}\rangle$, calculated by dividing the total simulation time by the number of barrier crossings, are tabulated together with the correlation times, calculated with eq 4, for Ala and Leu methyls in Tables 1 and 2. For a methyl group undergoing three-site jumps, the correlation time (τ) is related to the residence time via $\tau = {}^2/_3\langle\tau_{res}\rangle$ when the correlation function is well converged.

The N−C_α−C_β−H1 dihedral angle, ϕ (H1 is one of the three methyl hydrogens, arbitrarily chosen but distinguishable in the simulation), is shown as a function of time in Figure 6 for four representative alanines of the liganded SNase simulation: A12 and A60, which have "fast-spinning" methyls with relatively well converged correlation functions; and A69 and A94, whose

Table 2. Leucine C_δ−H Relaxation Times τ (ps)[a]

		liganded			unliganded		
residue	methyl	τ_{exp}[b]	τ_{sim}[b]	$\langle t_{res}\rangle$[c]	τ_{exp}	τ_{sim}	$\langle t_{res}\rangle$
7	1	32(1)	29(2)	74	26(1)	23(4)	45
	2	33(1)	29(2)	63	45(6)	11(1)	29
14	1	52(4)	27(2)	53	55(3)	200(90)	400
	2	39(3)	160(3)	460	37(4)	58(14)	130
25	1	12(2)	19(1)	36	21(2)	16(2)	23
	2	28(2)	170(30)	250	34(2)	300(170)	330
36	1	53(1)	44(4)	73		55(13)	71
	2	26(1)	55(6)	140	24(1)	21(3)	39
37	1	80(3)	220(40)	350	48(2)	190(80)	400
	2	52(1)	420(120)	140	31(2)	77(21)	95
38	1	13(4)	380(100)	1100	23(1)	42(9)	91
	2	16(4)	130(20)	220	15(1)	74(20)	180
89	1	33(2)	56(6)	150	28(2)	65(17)	80
	2	6(1)	45(4)	51	4(1)	8(0.7)	11
103	1	57(2)	150(30)	200	64(2)	38(7)	43
	2	39(3)	84(10)	170		45(10)	67
108	1	24(3)	20(1)	41	32(2)	19(3)	27
	2	25(3)	33(3)	64	27(2)	15(2)	23
125	1	33(1)	94(12)	100	47(9)	150(60)	150
	2	14(1)	22(1)	52	32(1)	31(6)	38
137	1	24(1)	52(5)	110	23(1)	33(6)	83
	2	23(1)	18(1)	42	23(1)	14(2)	29

[a] Where there is no value for simulation, the correlation function was not sufficiently converged for calculation of τ. [b] τ_{exp} and τ_{sim} are the relaxation times from the experiment of Nicholson et al.[7] and simulation, respectively. Numbers in parentheses are one standard deviation as calculated by a Monte Carlo procedure for NMR data,[47] and estimates of the standard error from eq 5 for the simulation data. [c] $\langle\tau_{res}\rangle$ is the average time between rotations of a methyl across its 3-fold barrier in simulation.

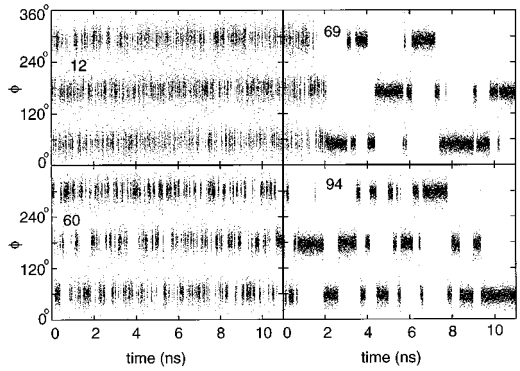

Figure 6. Time dependence of the N−C_α−C_β−H1 dihedral angle, ϕ, for four representative alanines, A12, A60, A69, and A94, during the simulation of liganded SNase.

methyls spin more slowly and therefore have correlation functions unconverged in the 11 ns of simulation. Figure 7 shows the C_β−H correlation functions for A12 and A60 in a and the corresponding C_α−C_β and C_α−H correlation functions in b.

Experimental[7] and simulated squared order parameters are plotted for Ala C_α−H and C_α−C_β bond vectors in Figures 8 and 9, respectively. The experimental error bars indicate one standard deviation as determined by a Monte Carlo approach.[7] Leu C_γ−C_δ squared order parameters are given in Table 3. NMR squared order parameters for Ala C_α−C_β and Leu C_γ−C_δ bond vectors were obtained by dividing the overall squared order parameters for methyl ^{13}C relaxation by 0.111, while simulated order parameters were obtained directly from motions of the corresponding C−C bonds.

Figure 10 compares the correlation of simulated Leu C_γ−C_δ squared order parameters, $S^2_{\gamma\delta}$, with predictions from the theoretical expression given by eq 12.

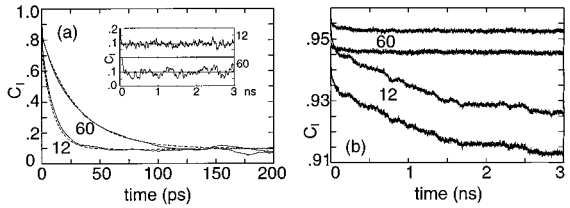

Figure 7. Correlation functions representative of Ala and Leu residues with fast relaxation times. For (a) $C_\beta-H$ and (b) $C_\alpha-H$ and $C_\alpha-C_\beta$ bonds of A12 and A60 (liganded SNase simulation). The solid lines are obtained directly from the simulation using eq 1, and the dashed lines are obtained using eq 14. The inset in a shows the long-time behavior of $C_I(t)$; straight lines are drawn at the values of S^2 calculated from the simulation: 0.0922 for A12 and 0.0961 for A60. The upper and lower curves of each pair of curves in b correspond to the $C_\alpha-C_\beta$ and $C_\alpha-H$ bonds, respectively.

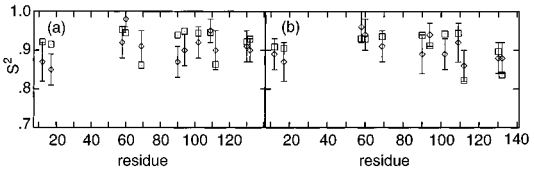

Figure 8. Squared generalized order parameters (S^2) for Ala $C_\alpha-H$ bonds. Diamonds and error bars at one standard deviation correspond to experiment;[7] squares correspond to simulation. (a) Liganded SNase. (b) Unliganded SNase.

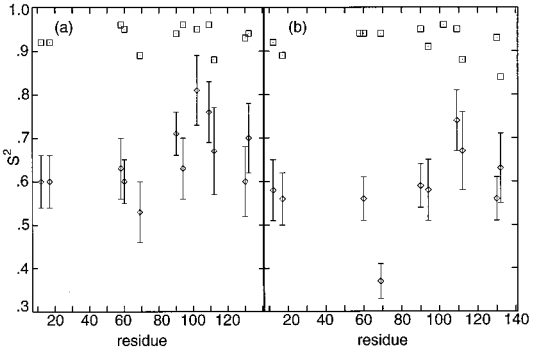

Figure 9. Squared generalized order parameters (S^2) for Ala $C_\alpha-C_\beta$ bonds. Diamonds and error bars at one standard deviation correspond to experiment;[7] squares correspond to simulation. Experimental values were calculated by dividing S^2 for $C_\beta-H$ vectors by 0.111, and simulation values were calculated directly from the dynamics of $C_\alpha-C_\beta$ bonds. (a) Liganded SNase. (b) Unliganded SNase.

For comparison with ideal tetrahedral geometry, which is assumed when a value of 0.111 for S^2_{rot} is used to compute S^2_{axis} from S^2 for methyl motions (eq 10), average methyl C−C−H angles (β) were calculated from simulation and compared with experimental and ab initio results. Values of β and corresponding values of S^2_{rot} are given in Table 4.

Finally, contributions of nonbonded hydrogens to selected order parameters, calculated with eq 7 but replacing $F(r)$ with $\hat{F}(r)$ (eq 8), are given in Table 5.

Discussion

Overall Structure and Fluctuations. Both simulations require a remarkably long equilibration. Figure 3 shows that during the 4-ns equilibration of liganded SNase, loop regions are most mobile, and small adjustments occur in the β-sheet regions, the two N-terminal helices, and the C-terminal helix. The simulated structure is very stable for the following 11 ns. The rmsd of the backbone heavy atoms vs the crystal structure during this period is 1.5 Å (see Figure 1) and vs the average simulated structure from the same period is only 0.5 Å. Differences between the hydrated and crystal structures may arise from, for example, crystal contacts, differing solvation levels, inaccuracies in the potential function, or absence of counterions in the simulation.

Unliganded SNase has a shorter initial equilibration, 1.75 ns. As discussed below, many data suggest that unliganded SNase is more flexibile than liganded SNase, and this enhanced flexibility may be responsible for the faster equilibration. The period used for analysis, 1.75−3.75 ns, is shorter than for liganded SNase largely because our primary interest was the liganded form. We note, though, that methyl rotations were on average somewhat faster in unliganded SNase, so that a shorter simulation was sufficient for a similar degree of convergence in side-chain methyl order parameters.

Fluctuations of the backbone during simulation (Figure 2) are of the same magnitude as fluctuations calculated from crystal

Table 3. Leucine $C_\gamma-C_\delta$ Order Parameters (S^2)[a,b]

		liganded		unliganded	
residue	methyl	exp	sim	exp	sim
7	1	0.53(5)	0.68[c]	0.40(4)	0.65[c]
	2	0.42(3)	0.26[c]	0.46(4)	0.59[c]
14	1	0.82(9)	0.88	0.81(6)	0.93
	2	0.65(6)	0.88	0.65(5)	0.93
25	1	0.79(8)	0.95	0.71(6)	0.94
	2	0.76(10)	0.93	0.82(6)	0.94
36	1	0.37(5)	0.62[c]		
	2	0.46(3)	0.52[c]	0.34(3)	
37	1	0.85(6)	0.95	0.63(6)	0.94
	2	0.74(5)	0.92	0.55(3)	0.92
38	1	0.64(9)	0.93	0.45(4)	0.93
	2	0.54(5)	0.89	0.35(3)	0.90
89	1	0.78(5)	0.90	0.57(4)	0.93
	2	0.88(9)	0.86	0.59(4)	0.92
103	1	0.85(6)	0.83	0.57(5)	0.82
	2	0.82(5)	0.74		0.74
108	1	0.72(6)	0.93	0.71(6)	0.92[c]
	2	0.78(6)	0.93	0.65(15)	0.92
125	1	0.46(3)	0.87	0.29(3)	0.85[c]
	2	0.39(3)	0.80	0.34(2)	0.81[c]
137	1	0.47(3)	0.88	0.40(4)	
	2	0.55(6)	0.83	0.51(7)	

[a] $C_\gamma-C_\delta$ squared order parameters were calculated directly for simulation and by dividing $C_\delta-H$ squared order parameters by 0.111 for experiment.[7] Numbers in parentheses are one standard deviation as calculated by a Monte Carlo procedure for NMR data.[47] [b] Where there is no value for simulation, the correlation function was not sufficiently converged for calculation of S^2. [c] The correlation function from which this value was computed is less well converged than the others.

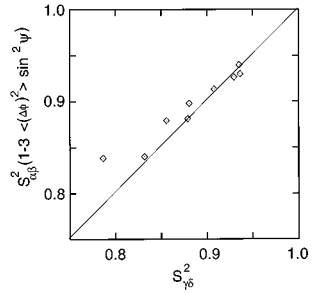

Figure 10. Theoretical value of $S^2_{\gamma\delta}$ from eq 12 vs $S^2_{\gamma\delta}$ calculated directly from motion of $C_\gamma-C_\delta$ bond vectors. From simulation of liganded SNase. Line is drawn to guide the eye; ordinate $S^2_{\gamma\delta}$ is averaged over both methyls of a given residue; and L7 and L36 are excluded, as they underwent dihedral angle (ϕ) transitions during simulation.

Table 4. Average Methyl Group C−C−H Angles (β, deg) and Corresponding Values[a] of S^2_{rot}

amino acid	minimization[b]	simulation		experiment[d]	ab initio[e]
		liganded[c]	unliganded[c]		
Ala	110.27 (0.102)	110.49 (0.100)	110.52	110.12 (0.104)	110.03 (0.105)
Leu	110.65 (0.098)	110.96 (0.095)	111.01		
Val	110.86 (0.096)	111.08 (0.094)	111.06	111.66 (0.088)	

[a] Values of S^2_{rot} from eq 10 corresponding to given angle are in parentheses. [b] From minimization of neutral amino acid in vacuo using parameter set PARM30 with reduced methyl torsional barriers. [c] Entries are averages over all methyls in residues of given type. [d] From neutron diffraction data for L-alanine[49] and L-valine.[50] [e] MP2/6-311++G(D,P) calculation.

Table 5. Percent Contribution[a] of Nonbonded Hydrogens to S^2 Calculated from NMR

residue	atom	total[b]	intraresidue[c]	extraresidue	
				$r < 5$ Å[d]	5 Å $< r <$ 7 Å[e]
A90	N	2.9[f]	1.6	1.2	0.1
	C_α	5.4	3.8	1.4	0.2
	C_β	9.3	5.7	2.8	0.8
L89	N	3.2	2.2	0.9	0.1
	C_α	6.5	5.4	0.9	0.2
	$C_{\delta1}$	10.2	8.4	1.1	0.7
	$C_{\delta2}$	13.0	9.6	2.6	0.8

[a] Based on simulation of liganded SNase. [b] Contribution from all hydrogens less than 7 Å from the heteronucleus. [c] Contribution from nonbonded intraresidue hydrogens. [d] Contribution from extraresidue hydrogens less than 5 Å from the heteronucleus. [e] Contribution from extraresidue hydrogens 5−7 Å from the heteronucleus. [f] Values are percentage of sum in eq 8 due to contributions from hydrogens corresponding to column heading.

structure temperature factors. In all cases, loop regions display greatest mobility, especially the one near residue 50. In simulation, unliganded SNase has slightly larger fluctuations than liganded SNase overall, and considerably larger fluctuations in particular regions. The most enhanced mobility of unliganded vis-á-vis liganded SNase is displayed by the loops containing residues 50, 85, and 115, and by the C-terminal end of helix 3. The latter two loops form the entrance to the ligand binding pocket, and helix 3 forms one side of the binding pocket. Thus the binding pocket is somewhat unstable in the unliganded simulation, consistent with unliganded SNase having greater flexibility in solution.

Backbone Dynamics. The simulated and experimental[6] backbone N−H order parameters shown in Figure 5 are generally consistent with the secondary structure, more motion being displayed in loops than in sheets or helices. For liganded SNase, agreement between simulation and experiment is on average quite good, the average value of N−H squared order parameters being 0.82 and 0.83, respectively. Except for five particularly large experimental values (for T22, V23, A60, F61, and Q123), a squared order parameter of ∼0.88 represents the maximum motional restriction experienced by N−H bond vectors in both simulation and experiment. In the cone model, this corresponds to motion of the N−H bond vector within a cone of semiangle 17°. Since residues with this mobility occur in regions of secondary structure, this probably represents the maximum motional restriction of a strong hydrogen bond. Simulated squared order parameters for C_α−H bond vectors display the same trends as those for N−H bond vectors but are on average 10% higher. A similar relationship between N−H and C_α−H order paramters has been noted by NMR for alanines in liganded and unliganded SNase.[7] From NMR data alone, it was uncertain whether variation in bond lengths might be responsible for the larger C_α−H order parameters,[7] but the simulation results suggest that the larger values are in fact indicative of slightly greater motional restriction.

N−H squared order parameters from simulation are on average 4% smaller in unliganded than in liganded SNase, suggesting that ligand binding renders SNase more rigid. This is consistent with trends in recently reported NMR order parameters for both forms of SNase,[8] as well as with the thermal unfolding and amide proton exchange data mentioned earlier.

To confirm that differences in simulation time and equilibration period did not influence these results, N−H order parameters were calculated for liganded SNase from the interval used for unliganded SNase, 1.75−3.75 ns. This period is characterized by greater backbone mobility for liganded SNase, as evidenced by Figures 1 and 3. The average N−H squared order parameter is 0.81 in the early interval, compared with 0.82 in the longer, later interval. We conclude that the 4% difference in N−H squared order parameters is not an artifact of incomplete equilibration.

Alanine Residues. Simulated and experimental[7] C_α−H squared order parameters, $S^2_{\alpha H}$, are in good agreement, having values typical of the backbone, ∼0.90 (Figure 8). The average values for liganded and unliganded SNase, respectively, are 0.91 and 0.90 for experiment and 0.92 and 0.91 for simulation. Simulated squared order parameters for C_α−C_β bond vectors ($S^2_{\alpha\beta}$), calculated directly from the motions of these bond vectors, are on average only 1% larger than the C_α−H squared order parameters.

Experimental values for $S^2_{\alpha\beta}$ were calculated by dividing the overall squared order parameter for the ^{13}C-labeled C_β by 0.111, as discussed above. In experiment, as in simulation, $S^2_{\alpha\beta}$ is somewhat smaller for unliganded than for liganded SNase (the experimental values range from 0.56 to 0.74 for unliganded and from 0.60 to 0.81 for liganded SNase). However, the experimental $S^2_{\alpha\beta}$, which average only 0.62, are much smaller than those from simulation or than the experimental $S^2_{\alpha H}$. It is difficult to understand how S^2 can be so much smaller for C_α−C_β than for C_α−H motions. Furthermore, simulation detects no large-scale motion of the C_α−C_β bond axis, although the experimental relaxation times are of the order of 10 ps (see Table 1), well within the time scale accessible to simulation. It has been suggested that deviations of the methyls from ideal tetrahedral geometry, which would alter the scaling factor of 0.111, may be responsible for the surprisingly small values of $S^2_{\alpha\beta}$ reported in Figure 9.[7] Some distortion does occur (see section on methyl geometry below), but it is not large enough to account for the difference between the C_α−H and C_α−C_β order parameters measured by NMR. We also investigated the commonly made assumption that using average bond lengths and ignoring the influence of nonbonded hydrogens on spin relaxation (eq 7) introduces negligible error. We found (see the later section on the tests of these assumptions) that using average bond lengths influences squared order parameters insignificantly and that ignoring the influence of nonbonded hydrogens causes the difference between $S^2_{\alpha\beta}$ and $S^2_{\alpha H}$ to be

*under*estimated. Thus the discrepancy between simulation and NMR in regard to $S^2_{\alpha\beta}$ remains unresolved.

Relaxation times τ for all alanines are given in Table 1. Five of the alanines had well-converged correlations functions and standard errors in τ less than 5 ps (A12, A60, A90, A130, and A132). For these five alanines, the average τ for liganded and unliganded SNase, respectively, was 31 and 35 ps for experiment and 32 and 24 ps for simulation, suggesting that the rotational barrier heights and the simulated dynamics of methyl groups are realistic. However, trends from residue to residue are inconsistent.

Several of the alanines have relaxation times much greater in simulation than in experiment. This is particularly true of liganded SNase; the corresponding relaxation times for unliganded SNase tend to be smaller (particularly for A58, A94, and A109), consistent with unliganded SNase having greater flexibility. In its simulated conformation, liganded SNase has less side-chain flexibility than in the experimental conformation, so that in simulation some methyls become "locked" into place and cannot spin. One possible explanation, suggesting further research, is that on the NMR time scale a number of microstates are sampled, while on the shorter time scale of simulation only one microstate is sampled. We note in this regard that Ala69 samples two different environments during simulation, one in which it rotates quickly (the first 2 ns of simulation), and one in which it rotates slowly (the latter 9 ns), as Figure 6 demonstrates. That this is the only such occurrence during the simulation suggests that such microstates may exist but not be reflected in the simulated relaxation times. Of course, whether the approximate nature of the potential functions or the limited degree of solvation in simulation induces rigidity or compacting of the enzyme remains to be investigated.

To assess possible differences between the X-ray structure and simulations, barriers to methyl rotation in the crystal structure were calculated and compared with the simulated dynamics. Barrier heights were calculated by energy minimizing the hydrated crystal structure, rotating the methyls by 60°, and re-energy-minimizing with the N−C_α−C_β−H1 dihedral angle restrained. The barrier heights, calculated as the energy difference between the two energy-minimized structures, range from 3.9 kcal/mol for A94 to 8.3 kcal/mol for A102. Of the 12 alanines, six have barrier heights greater than 5.5 kcal/mol, and only one of these has a relaxation time smaller than 100 ps. Likewise, of the six alanines with barrier heights less than 5.5 kcal/mol, only one has a relaxation time greater than 100 ps. Thus, although barrier heights will vary as the protein conformation changes during simulation, the crystal structure appears to be representative of the range of environments experienced by the alanine methyls. [The simulated rotation rates differ by up to 150-fold (τ (A109)/τ (A12) = 150), while the largest difference in barrier heights corresponds to a 2600-fold difference in rotation rate. Presumably the range of conformations accessed during simulation accounts for the order of magnitude difference.] van der Waals interactions are the predominant contributor to variation in barrier heights. The maximum van der Waals contribution to the difference between two barrier heights was 3.6 kcal/mol, followed by bond angle terms (1.6 kcal/mol) and electrostatic terms (1.6 kcal/mol). We conclude that the variation in simulated methyl rotation rates is predominantly a steric effect.

The correlation functions for A12 and A60, shown in Figure 7, were compared with a theoretical expression involving k, the rate for methyl rotational transitions about the C_3 symmetry axis:

$$C_l(t) = S^2_{\alpha\beta}[P_2^2(\cos\beta) + (1 - 3\langle(\Delta\phi)^2\rangle \sin^2\beta - P_2^2(\cos\beta))e^{-3kt}] \qquad (14)$$

which is valid for times greater than a few picoseconds. In eq 14, $\langle(\Delta\phi)^2\rangle$ is the mean square fluctuation of the N−C_α−C_β−H dihedral angle excluding jumps between wells (i.e., in averaging, the value of ϕ modulo 120° was used so that $\langle(\Delta\phi)^2\rangle$ reflects only motions within wells and not transitions between wells), β is the average C_α−C_β−H angle (110.6° for both methyls), $S^2_{\alpha\beta}$ is the squared order parameter for the methyl symmetry axis, and k is obtained from an exponential fit to the number correlation function for jumps between the wells. As can be seen in Figure 7, considering that no adjustable parameters were used, the agreement is impressive. In particular, the initial drop to about 0.8 is reproduced, demonstrating that it is a consequence of rapid librations of both the C_β−H and C_α−C_β vectors. The values of k obtained from the number correlation function and used in eq 14, 0.033 ps^{-1} for A12 and 0.011 ps^{-1} for A60, are in good agreement with values obtained from the average residence times, 0.036 ps^{-1} and 0.14 ps^{-1}, respectively, using the relationship $\langle\tau_{res}\rangle = 1/(2k)$. Furthermore, integrating eq 4 using eq 14 for $C_l(t)$ and the values for k given above yields relaxation times of 7.2 ps for A12 and 25 ps for A60, which compare well with the values of 7.5 and 23 ps obtained directly from the simulation with eqs 1, 3, and 4 (Table 1).

Leucine Residues. Leucine order parameters for the side-chain C−C bond vectors decrease with increasing distance from the backbone, consistent with mobility increasing as one moves out the side chain. The average values of the C_α−C_β, C_β−C_γ, and C_γ−C_δ squared order parameters are 0.959, 0.934, and 0.882, respectively (excluding residues 7 and 36, whose C_γ−C_δ order parameters could not be estimated accurately as a consequence of rare dihedral transitions).

We focus on C_γ−C_δ and C_δ−H order parameters because the available NMR data[7] is for δ carbons. Simulated C_γ−C_δ order parameters calculated for the 11 leucine residues are in the range 0.74−0.95, excepting four whose correlation functions were not well converged (Table 3). The average value is 0.88 for liganded SNase and 0.90 for unliganded SNase (averaged over the 18 cases for liganded SNase and 13 cases for unliganded SNase in which $C_l(t)$ was converged). These are in same range as the values for backbone N−H and C_α−H vectors and in the cone diffusion model correspond to a semiangle of 15−17°. The experimental values were obtained from a fit of the data by a functional form appropriate for two motions, one fast and one slow.[5,6] The fast motions were assumed to correspond primarily to methyl rotations, so a value of 0.111 for the corresponding squared order parameter, S^2_{rot}, was used in the fit. Order parameters for the slow motions, which probably correspond to reorientation of the C_β−C_γ axis, are given in Table 3.

Relaxation times for the fast motions are of the order of 10 ps and are given in Table 2. Relaxation times for the slow motions have large uncertainties and are not given, but they are generally larger than about 2 ns.[5,6] Motions having this time scale occur too infrequently in the 3.75- and 18-ns simulations to generate adequate sampling statistics. In fact, 60° transitions of the dihedral angle ϕ are observed only for leucines L7 and L36 in the liganded SNase simulation, and their frequency is too small to generate converged correlation functions. The other leucines manifest no ϕ transitions during the liganded SNase simulation, so their order parameters reflect only fast librations. This is probably why the experimental order parameters, which reflect both slow and fast motions, are

generally smaller. It has been demonstrated that populating a second dihedral state more than 20% of the time will decrease $S^2_{\gamma\delta}$ from the simulated values to the range of NMR.[5,6]

Figure 10 demonstrates that the simulated $C_\gamma-C_\delta$ order parameters are in agreement with the theoretical expression given by eq 12, which relates $S^2_{\gamma\delta}$ to librations of the side chain when dihedral transitions about a C−C bond do not occur. Furthermore, we find that $S^2_{\gamma\delta}$ is linearly correlated with $\langle(\Delta\phi)^2\rangle$, so scatter in the plot is due mainly to the other factors in eq 12. Since the NMR Leu side-chain relaxation times in Table 2 reflect the faster motions but not the slow dihedral transitions,[7] it is meaningful to compare these relaxation times with those from simulation. As for the alanines, some of the simulated leucine methyls spin with relaxation times close to the experimental values, and some spin much more slowly. Excluding methyls for which either the liganded or unliganded relaxation time exceeds the largest experimental value, 80 ps, the average value of τ for liganded and unliganded SNase is, respectively, 22 and 25 ps for experiment and 34 and 23 ps for simulation. Most of the relaxation times that are very long in the liganded simulations are reduced in the unliganded simulations. These values for simulation are consistent with increased side-chain flexibility for unliganded SNase, while the ones for experiment suggest reduced flexibility.

Methyl Geometry. Although the experimental Ala $C_\alpha-C_\beta$ and Leu $C_\gamma-C_\delta$ order parameters depend on $S^2_{\rm rot}$, the correct value for $S^2_{\rm rot}$ is not precisely known. The theoretical value for ideal tetrahedral geometry is 0.111, as mentioned above, but methyl groups in proteins may deviate from this gemetry. Single-crystal neutron diffraction studies of L-alanine report methyl C−C−H angles, θ, of 110.03°,[49] and similar studies of L-valine report θ values of 111.88° and 111.42° for the γ^1 and γ^2 methyls, respectively.[50] Values of $S^2_{\rm rot}$ calculated from these numbers are up to 23% smaller than the ideal value of 0.111. A value of 0.111 for $S^2_{\rm rot}$ was nevertheless used to extract values for $S^2_{\alpha\beta}$ (alanine) and $S^2_{\gamma\delta}$ (leucine) from the NMR data.[5,6]

Table 4 reports the average value of θ and the corresponding value of $S^2_{\rm rot}$ for alanine, leucine, and valine from various experimental and theoretical data. Average values of θ from simulations of liganded and unliganded SNase are in excellent agreement. Ab initio and neutron diffraction data for alanine are in excellent agreement, the predicted values of θ differing by only 0.09°. (Note that the environments differ, the former being vacuum and the latter being an L-alanine crystal.) Minimization of neutral alanine in vacuo with CHARMM predicts a θ 0.13° larger than the ab initio calculations or experiment. Thus CHARMM appears to slightly overestimate θ for alanine. On the other hand, relative to experiment, CHARMM underestimates θ for valine (note again that the environments differ). The simulation values of θ for all three residues are larger than the minimized CHARMM values by 0.20−0.31°, suggesting that at 300 K, the hydrogens tend to open to a slightly larger angle due to anharmonic effects. Values of θ—whether from minimization, simulation, or experiment—increase from alanine to leucine from valine. This trend is consistent with variation in θ being a steric effect.

It is clear from Table 4 that for alanine, leucine, and valine, 0.111 is too high a value for $S^2_{\rm rot}$, and the appropriate value varies with the type of residue. Simulation and experiment suggest a value for alanine of between 0.100 and 0.104 and a value for residues with more steric hindrance, such as leucine and valine, at least 0.005 smaller. The use of these values would increase the experimental $C_\alpha-C_\beta$ squared order parameters in Figure 9 by only about 10%. Thus the discrepancy between theory and experiment remains.

Finally, with the simulation we can test the validity of eq 11, which is used to determine the order parameter of the Ala $C_\alpha-C_\beta$ bond from the methyl $C_\beta-H$ order parameter. Recall that this equation is based on the assumption that the motions of and about the symmetry axis of the methyl group are independent and axially symmetric. For A12, A60, A90, A130, and A132, whose $C_\beta-H$ correlation functions are converged in the simulation of liganded SNase, the average value of the ratio $S^2_{\beta H}/S^2_{\alpha\beta}$ is 0.096 ($S^2_{\beta H}$, the $C_\beta-H$ squared order parameter, varied between 0.085 and 0.098, while $S^2_{\alpha\beta}$ varied between 0.93 and 0.95). For these residues the average value of the angle between the $C_\alpha-C_\beta$ and $C_\beta-H$ bonds yielded an "average" $S^2_{\rm rot}$ of 0.099, in good agreement with the above ratio. Thus the discrepancy between theory and experiment does not appear to arise from the breakdown of eq 11.

Tests of Some Assumptions in Analysis of NMR Measurements. As discussed previously, NMR order parameters actually correspond to the quantity $\hat{S}$ (from eqs 6 and 7, ignoring any influence from nonbonded hydrogens) rather than to S (from eq 2 or eq 3). To determine the magnitude of the error introduced by interpreting $\hat{S}^2$ as S^2, we calculated both for the simulation of liganded SNase.[51] The average of the magnitude of the error is 0.017% for backbone N−H and C−H squared order parameters, so we conclude that using average bod lengths to calculate generalized order parameters from NMR relaxation times and nuclear Overhauser effects introduces negligible error. We note in this regard that the $C_\alpha-H$ and $C_\beta-H$ bond lengths used in the PARM30 parameter set and those obtained from ab initio calculations for neutral alanine compare favorably, ruling out bond length as a significant contributor to the difference between $S^2_{\alpha\beta}$ values from simulation and NMR. The bond lengths are 1.09 Å in the PARM30 parameters set, and optimized MP2/6-31++G(D,P) calculations yield 1.095 Å for the $C_\alpha-H$ bond length and 1.092, 1.092, and 1.096 Å for the $C_\beta-H$ bond lengths.

In analyzing order parameters from NMR relaxation data, it is commonly assumed that only hydrogens bonded directly to the heteronucleus contribute importantly to the NMR signal. This assumption is implicit in eqs 6 and 7. To judge the limitations of this assumption, simulated order parameters corresponding more precisely to those extracted from NMR measurements were calculated by including the influence of nonbonded protons on the NMR signal via eq 8. Calculations were made for two residues near the center of mass of SNase, L89 and A90, for the liganded SNase simulation. As Table 5 demonstrates, including nonbonded hydrogens increases S^2 by 3% for backbone nitrogens, 5−7% for α-carbons, and 9−13% for side-chain methyl carbons as compared with the directly bonded values. The larger methyl figure (13%) corresponds to leucine. Of these amounts, roughly two-thirds is due to nonbonded intraresidue hydrogens, and most of the rest is due to extraresidue hydrogens within 5 Å. The difference between the backbone atoms and the side-chain methyls reflects the greater proximity of side chain methyl carbons to both intra- and extraresidue hydrogens. These calculations suggest that

(49) Lehmann, M. S.; Koetzle, T. F.; Hamilton, W. C. *J. Am. Chem. Soc.* **1972**, *94*, 2657.

(50) Koetzle, T. F.; Golic, L.; Lehnmann, M. S.; Verbist, J. J.; Hamilton, W. C. *J. Chem. Phys.* **1974**, *60*, 4690.

(51) The minima in the PARM30 harmonic potentials for backbone N−H and C−H bonds occur at 1.00 and 1.09 Å, respectively, and the force constants are 340.0 and 400.0 kcal/mol·Å^2.

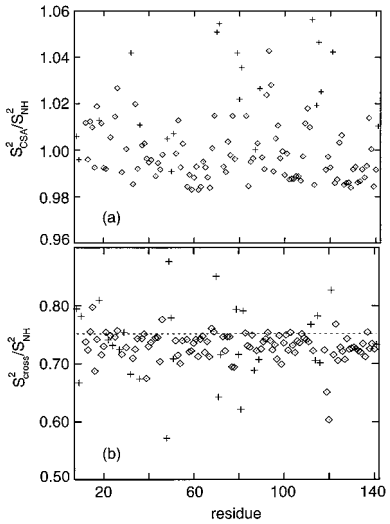

Figure 11. (a) Ratio of the squared order parameter for the CSA vector, S^2_{CSA}, to the squared order parameter for the backbone N−H bond vector, S^2_{NH}, for all residues except prolines. (b) Ratio of the cross correlation squared order parameter, S^2_{cross}, to S^2_{NH}. The horizontal line indicates the theoretical value, $P_2(\cos\chi)$, for $\chi = 24°$. Diamonds designate residues for which $S^2_{NH} \geq 0.8$, and plusses designate others.

bond vector squared order parameters extracted from NMR may be too high by the amounts mentioned above. We note that, for alanine, nonbonded hydrogens are more important for $^{13}C_\beta$ than for $^{13}C_\alpha$ spin relaxation. Therefore the bond vector order parameters calculated from NMR are overestimated by more for $C_\alpha-C_\beta$ bonds than for $C_\alpha-H$ bonds, which effectively *increases* the discrepancy between simulation and NMR by up to 4%.

^{15}N relaxation times are influenced by the chemical shift anisotropy (CSA) as well as by the dipolar interaction. The order parameter for the ^{15}N CSA autocorrelation is usually assumed to be identical to that for the $^{15}N-^1H$ dipolar interaction. This assumption was tested with the liganded SNase simulations. The CSA for ^{15}N relaxation is described by a unit vector in the C′−N−H plane making an angle of 24° with the N−H vector and pointing toward the N−C′ vector.[52] Order parameters for the CSA vectors, S_{CSA}, were calculated and compared with those for N−H bond vectors, S_{NH}. The ratio S^2_{CSA}/S^2_{NH} is shown by residue in Figure 11a. This ratio varies between 0.98 and 1.06 and is less than 1.02 for most residues. (If it seems counterintuitive that S^2_{CSA} and S^2_{NH} can differ, consider the simplified case in which the only motion of these vectors is rotation about the C−N axis. The order parameters would clearly differ since the two vectors make different angles with the C−N axis.)

A method for measuring the cross correlation between the $^{15}N-^1H$ dipolar interaction and the ^{15}N CSA from NMR data has recently been described.[46] To assess assumptions made in analyzing results obtained using this method, we computed S^2_{cross}, which corresponds to the long-time limit of the correlation function

$$C_I(t) = \langle P_2(\hat{\mu}_{NH}(\tau)\cdot\hat{\mu}_{CSA}(\tau + t))\rangle \qquad (15)$$

The ratio S^2_{cross}/S^2_{NH} is shown in Figure 11b. If the overall rotational diffusion of a macromolecule is isotropic and if internal motions are small and satisfy specific criteria including independence, this ratio is $P_2(\cos\chi)$, where χ is the angle between the N−H and CSA bond vectors.[46] This yields 0.752 for a χ of 24°. The values from simulation range from 0.60 to 0.80, but most cluster between 0.70 and 0.75.

Conclusion

An 11-ns segment of an 18-ns MD simulation of liganded SNase was used to calculate order parameters and correlation times associated with backbone N−H and $C_\alpha-H$ vectors as well as methyl C−H vectors of alanines and leucines. The backbone N−H order parameters are smaller than the corresponding $C_\alpha-H$ order parameters, in agreement with experiment. On average, the experimental and simulated backbone flexibility are similar, but there are differences on a residue-by-residue basis. Motional parameters calculated from a 2-ns segment of a 3.75-ns MD simulation of unliganded SNase are indicative of greater flexibility than those for liganded SNase, which is physically reasonable and consistent with some experimental data.

Simulation predicts a much larger dynamic range in the rates of methyl rotations than is observed experimentally. For methyl groups that are rapidly rotating in the simulation, there is satisfactory agreement with correlation times extracted from experiment. However, in the simulation there are a number of methyl groups that reorient so slowly that the number of transitions in 11 ns is insufficient to quantitate their correlation times. This discrepancy may reflect a difference in the NMR and simulation time scales, with several microstates being sampled in the former but not in the latter. Of course, it may also result from the approximate nature of the potential functions or the limited degree of solvation employed in the simulation. Further work is needed to address this issue.

Perhaps the most puzzling discrepancy between simulation and experiment involves order parameters of the $C_\alpha-C_\beta$ bond of alanines. Excluding terminal residues, the average experimental $S^2_{\alpha\beta}$ (found using eq 11) is 0.65, which is about 30% smaller than the average of the corresponding $S^2_{\alpha H}$. On the other hand, the simulation predicts that $S^2_{\alpha H} \cong S^2_{\alpha\beta} \cong 0.9$. This is physically reasonable since one expects the amplitude of the motion of the $C_\alpha-H$ and $C_\alpha-C_\beta$ bonds to be very similar. Interestingly, the same discrepancy was found in the very first comparison between simulation and experiment, performed by Lipari et al.[10] These authors found that the alanine $C_\alpha-C_\beta$ order parameters in BPTI, calculated from the original McCammon−Karplus 96-ps trajectory,[53] were much larger than those extracted from the ^{13}C relaxation experiments of Richarz et al.[54] At that time, because of the unavailability of $C_\alpha-H$ relaxation data for individual alanines and the shortness of the simulation, one could only conclude that the simulation underestimated the motional amplitudes. However, one must now seriously consider the possibility that it is the "experimental" order parameters that, for some reason, are too small and that the simulation gives a more accurate picture of the motional amplitudes of these vectors.

The experimental $S^2_{\alpha\beta}$ are obtained from $S^2_{\beta H}$ using eq 11, which assumes that the motions of and about the $C_\alpha-C_\beta$ axis are independent and axially symmetric. For rapidly rotating methyl groups, we have demonstrated the validity of this relation by simply calculating both sides of the equation from the simulation. To use eq 11 one needs S^2_{rot}. For ideal tetrahedral geometry, $S^2_{rot} = 0.111$, the value used by Nicholson et al. On the basis of ab initio molecular orbital calculations, we found

(52) Hiyama, Y.; Niu, C.-H.; Silverton, J. V.; Bavoso, A.; Torchia, D. A. *J. Am. Chem. Soc.* **1988**, *110*, 2378−2383.

(53) Karplus, M.; McCammon, J. A. *Nature* **1979**, *277*, 578.

(54) Richarz, R.; Nagayama, K.; Wüthrich, K. *Biochemistry* **1980**, *19*, 5189−5196.

that S^2_{rot} should be about 10% smaller. Such a value agrees with that calculated from the neutron diffraction geometry of alanine and was in fact used by Lipari et al. in analyzing the BPTI data. Thus it appears that this nonideal geometry effect helps but is not large enough to account for the difference between the experimental and simulated $C_\alpha-C_\beta$ order parameters. Furthermore, we found that using average bond lengths to calculate order parameters from NMR has insignificant influence of $S^2_{\alpha\beta}$, and including the effect of nonbonded hydrogens on spin relaxation would actually lead to a larger difference between simulation and NMR.

Thus we are left with the possibility that either the $S^2_{\beta H}$ extracted from the relaxation parameters are too small because of uncertainties in the overall correlation time, or the measured relaxation parameters are themselves inaccurate because of the rather complicated spin dynamics of $^{13}CH_3$. In this regard, we should mention that preliminary relaxation studies of deuterated alanine methyls in unliganded SNase performed in Lewis Kay's group (personal communication) yield $C_\alpha-C_\beta$ order parameters significantly larger than those obtained from ^{13}C relaxation. On the basis of these considerations, it would appear to be worthwhile to experimentally reexamine alanine $^{13}CH_3$ relaxation in both BPTI and SNase using both sophisticated two-dimensional as well as conventional one-dimensional techniques.

Acknowledgment. The authors thank Milan Hodošček for performing ab initio calculations and Dennis Torchia and Linda Nicholson for helpful discussions and providing NMR relaxation data. Time provided by the Computational Bioscience and Engineering Laboratory on their Intel iPSC/860 computer is gratefully acknowledged.

Appendix

Methyl Torsional Parameters. In preliminary simulations, the spin rates of Ala and Leu methyl groups were much too small. The average time between crossings of the 3-fold rotational barrier was 350 ps, whereas the average relaxation time τ for SNase Ala and Leu methyl C−H bond vectors measured by NMR is 30 ps. This suggested that the methyl rotational barriers of the parameter set PARM30 were too high and should be corrected.

Ab initio calculations were performed for neutral Ala in vacuo to assess the correct value of the methyl rotational barrier (Table 6). As the level of theory is increased, the barrier height for methyl rotation converges toward 3.4 kcal/mol, the experimental barrier for butane.[55] At the highest level of theory used, MP2/6-311++G(D,P), the barrier height is 3.38 kcal/mol.

Table 6. Ab Initio Barrier Heights for Neutral Ala Methyl Rotation in Vacuo

method	barrier (kcal/mol)
RHF/STO-3G	3.0
RHF/6-31G	3.6
RHF/6-311++G(D,P)	3.55
MP2/6-311++G(D,P)	3.38

For comparison, the effective PARM30 methyl rotational barrier was calculated by rotating the Ala methyl in increments of 5° and energy minimizing at each step with the $N-C_\alpha-C_\beta-H$ dihedral angle restrained. A barrier of 4.85 kcal/mol was obtained at a dihedral angle of 60° with respect to the staggered conformation. The contributions to the barrier were 3.17, 1.09, 0.37, 0.15, and 0.07 kcal/mol for the torsion, van der Waals, angle, bond, and electrostatic terms, respectively. Analogous calculations for the Ala methyl groups in liganded SNase yielded barriers of 5.4−8.3 kcal/mol, the dominant contributions being the torsion (2.9−3.4 kcal/mol) and van der Waals (0.7−3.5 kcal/mol) terms. In the SNase calculations, the positions of atoms more than 4 Å from the methyl group were fixed during minimization. In CHARMM, torsional potentials have the form

$$E_\phi = |k_\phi| - k_\phi \cos(3\phi) \tag{16}$$

where ϕ is the torsion angle and k_ϕ is a force constant. In PARM30, the barrier for Ala and Leu methyl rotations is provided by a torsional term with a k_ϕ of 1.6 kcal/mol. The rotational barrier would be 3.2 kcal/mol if the only contribution were the torsional term, but as seen above, other contributions are also important, especially the van der Waals terms.

On the basis of this analysis, the methyl torsional barrier was lowered by 1.6 kcal/mol by reducing k_ϕ from 1.6 to 0.8 kcal/mol. The effective barrier to methyl rotation for neutral Ala, recalculated with restrained minimization, is 3.40 kcal/mol, in agreement with the ab initio barrier. The reduced k_ϕ was used for Ala, Leu, Ile, Thr, and Val methyls in the simulations reported here.

JA972215N

(55) Durig, J. R.; Craven, S. M.; Harris, W. C. In *Vibrational Spectra and Structure, A Series of Advances*.; Durig, J. R., Ed.; Marcel Dekker: New York, 1972; Vol. 1, pp 23−176.